International Journal of Heat and Mass Transfer 52 (2009) 5064–5071

Contents lists available at ScienceDirect

International Journal of Heat and Mass Transfer

journal homepage: www.elsevier.com/locate/ijhmt

Conduction and radiation in a rectangular isotropic scattering medium with black surfaces by the RTNAM

Jian-Feng Luo *, Sheng-Li Chang, Jian-Kun Yang, Jun-Cai Yang

Department of Physics, National University of Defense Technology, 410073 Changsha, People's Republic of China

ARTICLE INFO

Article history:
Received 17 September 2008
Received in revised form 22 April 2009
Accepted 27 April 2009
Available online 18 June 2009

Keywords:
Ray tracing-node analyzing method
2-D rectangular medium
Isotropic scattering
Semitransparent medium
Transient

ABSTRACT

The ray tracing-node analyzing method (RTNAM) has been successfully developed to solve 1-D coupled heat transfer in isotropic and anisotropic scattering media in the past, and in this paper it is further extended to solving the 2-D coupled heat transfer in a rectangular isotropic scattering medium. Using the control-volume method, the partial transient energy equation is discretized in implicit scheme. The effect of radiation on heat transfer is considered as a radiative source term (RST) in the discretized energy equation, and in combination with spectral band model, the RST is calculated using the radiative transfer coefficients (RTCs), which are deduced by the ray tracing method. The Patankar's linearization method is used to linearize the RST and the opaque boundary condition, and the linearized equations are solved by the ADI method. Before solving the RTCs for isotropic scattering media, the RTCs without considering scattering must be solved at first. And then, the RTCs without considering scattering are normalized according to their integrality relationships. In addition, the correctness of the results obtained by the RTNAM is validated, and effects of scattering albedo and refractive index on transient temperature distribution are investigated.

1. Introduction

Semitransparent media has extensive engineering application, such as heat insulating techniques for the protection of aeroengines [1], manufacture and heat processing of glass products and its application in high-temperature environment [2], ignition and flame spread of semitransparent solids [3], optical window for spacecraft [4], etc. Almost all of the problems encountered in engineering applications are three-dimensional. For example, in optics field, temperature distribution within optical components, such as convex lens and concave lens, etc., will intensively affect the quality of image, especially when the optical system is installed in satellite. Thus, performing thermal analysis on multi-dimensional problems has a practical significance.

Using various methods, many researchers studied 2-D coupled radiative and conductive heat transfer in a semitransparent medium of various geometry. First of all, coupled heat transfer in a rectangular medium was studied most. Mishra et al. [5–8] investigated 2-D coupled heat transfer in a rectangular scattering semitransparent medium. In 2003, using the collapse dimension method (CDM) and the discrete transfer method (DTM) to solve the radiative transfer equation, they [5] evaluated the performance of the CDM and the DTM in terms of computational time and their ability to provide accurate results. In Ref. [6], the performance of computational cost of the Lattice Boltzmann method (LBM) and the finite volume method (FVM) were compared. In Ref. [7], they studied the effect of temperature dependent thermal conductivity on temperature distribution. In Ref. [8], using the FVM and the LBM, Mishra et al. studied the transient conduction and radiation. In 2004, Furmanski and Banaszek [9] proposed a new method based on the finite element spatial discretization combined with the iterative technique to study transient coupled radiative and conductive heat transfer in a rectangular medium. In 1991, Kim and Baek [10] studied coupled radiative and conductive heat transfer in a 2-D anisotropically scattering semitransparent rectangular enclosure using the discrete ordinates method (DOM). In the work of Viskanta and Lee [11], using DOM combined conduction and radiation in a 2-D glass rectangular medium was investigated. In 2002, Lacroix et al. [12] studied coupled radiative and conductive heat transfer in a silica rectangular semitransparent medium irradiated under a specific direction. In 2004, Mahapatra and Mahapatra [13] studied coupled radiative and conductive heat transfer in an isotropic scattering square enclosure using the DOM. In 2006, Lacroix et al. [14] analyzed transient coupled radiative and conductive heat transfer in nongray semitransparent 2-D rectangular media with mixed boundary conditions.

Optical components of cylinder shape have been widely used in laser field, so Wu and Wu [15,16] investigated 2-D transient radiative heat transfer in a length-limited cylinder using integration method, while Liu and Tan [17] used the DOM. In 1996, using

* Corresponding author.
E-mail address: Luo_jianfeng@yahoo.com (J.-F. Luo).

0017-9310/$ - see front matter © 2009 Elsevier Ltd. All rights reserved.
doi:10.1016/j.ijheatmasstransfer.2009.04.032

Nomenclature

$A_{k,T}$	$\int_{\Delta\lambda_k} I_{\lambda,b}(T)d\lambda/(\sigma T^4)$, where $I_{\lambda,b}(T)$ is the Plank's law, λ is the wavelength and subscript k means the kth spectral band
H_x	length of the rectangular medium (Fig. 1 (a)) (m)
H_x^*	dimensionless length of the rectangular medium, H_x/L_r
H_y	width of the rectangular medium (Fig. 1(a)) (m)
H_y^*	dimensionless width of the rectangular medium, H_y/L_r
h_i	convective heat transfer coefficients at surfaces S_i (W m^{-2} K^{-1}), where i = 1–4
(i,j)	node in medium, where i and j are the integral coordinates of each node along x direction and y-direction (Fig. 1(a)), respectively
k	thermal conductivity of medium (W m^{-1} K^{-1})
L_i	distance form surface S_i to black surrounding surface $S_{\infty i}$ (m), where i = 1–4
L_r	reference distance (m)
M	integer parameter, used to divide H_x into M equal parts
N	integer parameter, used to divide H_y into N equal parts
	conduction-radiation parameter of medium, $k/(4\sigma T_r^3 L_r)$
n_k	kth spectral band refractive index of medium
NB	total number of spectral bands
$S_{\infty i}$	black surface representing the surroundings (Fig. 1(a)), where i = 1–4
S_∞	enclosed black surroundings composed of $S_{\infty 1}$, $S_{\infty 2}$, $S_{\infty 3}$ and $S_{\infty 4}$
S_i	black boundary surface (Fig. 1(a)), where i = 1–4
$S_{i,j}$	boundary node j on surface S_i
T	absolute temperature (K)
T_0	uniform initial temperature (K)
T_r	reference temperature (K)
T^*	dimensionless temperature, T/T_r
$T_{S_{i,j}}$	temperature of boundary node j on surface S_i (K), where i = 1–4
$T_{\infty i}$	temperature of black surrounding surface $S_{\infty i}$ (Fig. 1(a)) (K), where i = 1–4
T_{gi}	gas temperature for convection at surface S_i (K), where i = 1–4
t_i	ith physical time (s)
t_i^*	ith dimensionless time, $4\sigma T_r^3 t_i/(\rho c L_r)$
$V_{(i,j)}$	control volume corresponding to node (i, j)
x	x-coordinate (m)
x^*	dimensionless coordinate, x/L_r
y	y-coordinate (m)
y^*	dimensionless coordinate, y/L_r
Δx	length of each control volume (m), H_x/M
Δy	width of each control volume (m), H_y/N
Δt_i	interval for time t_i (s)
Δt_i^*	dimensionless time interval for time t_i^*

Greek letters

α_k	kth spectral band absorption coefficient of medium (m^{-1})
η_k	kth spectral band absorption quotient of the attenuated energy of medium, $1-\omega_k$
κ_k	kth spectral band extinction coefficient of medium, $\kappa_k = \alpha_k + \sigma_k$ (m^{-1})
ρc	specific heat capacity of medium (J m^{-3} K^{-1})
σ	Stefan–Boltzmann constant, 5.6696×10^{-8} W m^{-2} K^{-4}
σ_k	kth spectral band scattering coefficient of medium (m^{-1})
ω_k	kth spectral band scattering albedo of medium, σ_k/κ_k

DOM, Vaillon et al. [18] studied radiative transfer in a 2-D gray medium confined between two coaxial infinitely long elliptic cylinders with black boundaries.

Industrial heat transfer problems at high temperature always deal with complex geometry, such as burners, kilns, boilers and combustion chambers, etc., and in these industrial applications, radiative heat transfer plays a predominant role. So, in 2004, using discrete transfer method (DTM) in combination with unstructured triangular meshes, Feldheim and Lybaert [19] studied radiative heat transfer in rather complex-shaped domains, such as quadrilateral cavity, L-shaped cavity and eccentric cylinders, and the ray effect of the DTM was studied. In 2007, they further developed a new FVM based on a cell vertex scheme and associated to a modified exponential scheme to study radiative [20] and transient coupled radiative and conductive [21] heat transfer in above complex-shaped domains as well as in cylindrical ring and elliptical ring domains, and in order to simplify the problems, the boundaries of those complex-shaped domains were considered to be black. In the work of Sakami et al. [22], the DOM was modified and applied to the study of coupled radiative and conductive heat transfer in semitransparent enclosures of arbitrary geometries.

The RTNAM was firstly proposed by Tan and Lallemand [23] in 1989, and 10 years later, it was extended to the isotropic scattering problem [24]. Recently, using this method Tan et al. [25–28] have studied the radiative heat transfer in an anisotropic scattering medium. Compared with other methods, such as the DOM and the FOM, etc., the RTNAM has its own advantages. For example, when solving radiative transfer equation, the radiative intensity does not need to be dispersed along the space coordinate, and the solid angle is not dispersed but is directly integrated. Thus, false scattering and ray effect will not exit in this method. So, the accuracy of this method is high in theory, and the results obtained by this method could be regarded as the benchmark. In the past, this method was mainly used to study 1-D problem [23–28]. Recently we have successfully extended this method to the 2-D coupled heat transfer problem in a rectangular absorbing medium [29], and based on this work, we further extend this method to the study of coupled heat transfer in a rectangular isotropic scattering medium in the present work.

2. Governing equation and opaque boundary condition

The physical model of present study is shown in Fig. 1 (a). As for inner node (i, j), the discretized form of the 2-D transient energy balance differential equation is

$$\rho c\left[T_{(i,j)}^{m+1}-T_{(i,j)}^{m}\right]\Big/\Delta t = k\left[T_{(i+1,j)}^{m+1}-2T_{(i,j)}^{m+1}+T_{(i-1,j)}^{m+1}\right]\Big/\Delta x^2 + k\left[T_{(i,j+1)}^{m+1}-2T_{(i,j)}^{m+1}+T_{(i,j-1)}^{m+1}\right]\Big/\Delta y^2 + \Phi_{(i,j)}^{r,m+1}/(\Delta x\Delta y), \quad (1)$$

where superscript m means the mth time increment. The term $\Phi_{(i,j)}^{r}$ is the RST of control volume $V_{(i,j)}$, which must be defined as the absorbed radiative energy by volume $\Delta x\Delta y$ (not by unit volume). $\Phi_{(i,j)}^{r}$ can be expressed as [23–29]

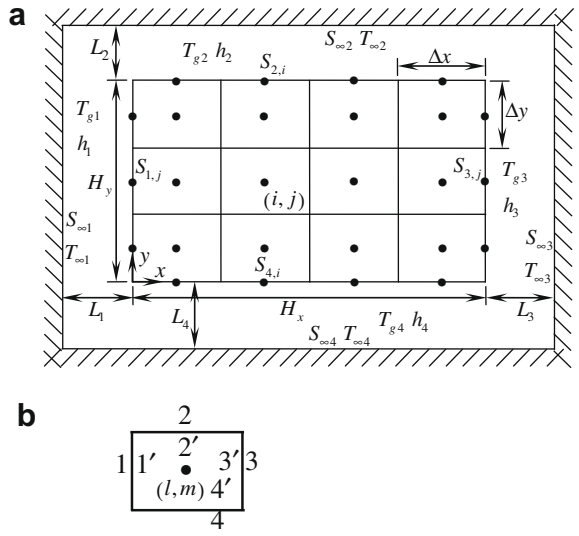

Fig. 1. Two-dimensional coupled heat transfer physical model. (a) Physical model. (b) Control volume.

$$\Phi^r_{(i,j)} = \frac{\sigma}{\pi}\sum_{k=1}^{NB}\left\{\sum_{m=1}^{N} n_k^2\left\{[S_{1,m}V_{(i,j)}]_k A_{k,T_{S_{1,m}}} T^4_{S_{1,m}} - [V_{(i,j)}S_{1,m}]_k A_{k,T_{(i,j)}} T^4_{(i,j)}\right\}\right.$$
$$+\sum_{m=1}^{N} n_k^2\left\{[S_{3,m}V_{(i,j)}]_k A_{k,T_{S_{3,m}}} T^4_{S_{3,m}} - [V_{(i,j)}S_{3,m}]_k A_{k,T_{(i,j)}} T^4_{(i,j)}\right\}$$
$$+\sum_{l=1}^{M} n_k^2\left\{[S_{2,l}V_{(i,j)}]_k A_{k,T_{S_{2,l}}} T^4_{S_{2,l}} - [V_{(i,j)}S_{2,l}]_k A_{k,T_{(i,j)}} T^4_{(i,j)}\right\}$$
$$+\sum_{l=1}^{M} n_k^2\left\{[S_{4,l}V_{(i,j)}]_k A_{k,T_{S_{4,l}}} T^4_{S_{4,l}} - [V_{(i,j)}S_{4,l}]_k A_{k,T_{(i,j)}} T^4_{(i,j)}\right\}$$
$$\left.+\sum_{l=1}^{M}\sum_{m=1}^{N} n_k^2\left\{[V_{(l,m)}V_{(i,j)}]_k A_{k,T_{(l,m)}} T^4_{(l,m)} - [V_{(i,j)}V_{(l,m)}]_k A_{k,T_{(i,j)}} T^4_{(i,j)}\right\}\right\}, \tag{2}$$

where $[V_{(i,j)}V_{(l,m)}]_k$, etc., are the spectral RTCs of isotropic scattering media. For example, $[V_{(i,j)}V_{(l,m)}]_k$ means the part of radiative energy absorbed by $V_{(l,m)}$ to that emitted from $V_{(i,j)}$ in the kth spectral band, and the meanings of the other RTCs are similar to that of $[V_{(i,j)}V_{(l,m)}]_k$.

Take $S_{2,i}$ as an example to illustrate the discretized opaque boundary condition, and then the heat balance at it can be expressed as

$$k\left(T_{(i,N)} - T_{S_{2,i}}\right)\Delta x/(\Delta y/2) + \left(q^r_{S_{2,i}} - q^r_{S_{2,i}\to S_\infty}\right) = h_2\left(T_{S_{2,i}} - T_{g2}\right)\Delta x, \tag{3}$$

where $q^r_{S_{2,i}}$ means the net radiative heat energy that all the nodes in the media transfer to $S_{2,i}$, and using RTCs it can be expressed as

$$q^r_{S_{2,i}} = \frac{\sigma}{\pi}\sum_{k=1}^{NB}\left\{\sum_{l=1}^{N} n_k^2\left\{[S_{1,l}S_{2,i}]_k A_{k,T_{S_{1,l}}} T^4_{S_{1,l}} - [S_{2,i}S_{1,l}]_k A_{k,T_{S_{2,i}}} T^4_{S_{2,i}}\right\}\right.$$
$$+\sum_{m=1}^{N} n_k^2\left\{[S_{3,m}S_{2,i}]_k A_{k,T_{S_{3,m}}} T^4_{S_{3,m}} - [S_{2,i}S_{3,m}]_k A_{k,T_{S_{2,i}}} T^4_{S_{2,i}}\right\}$$
$$+\sum_{l=1}^{M} n_k^2\left\{[S_{4,l}S_{2,i}]_k A_{k,T_{S_{4,l}}} T^4_{S_{4,l}} - [S_{2,i}S_{4,l}]_k A_{k,T_{S_{2,i}}} T^4_{S_{2,i}}\right\}$$
$$\left.+\sum_{l=1}^{M}\sum_{m=1}^{N} n_k^2\left\{[V_{(l,m)}S_{2,i}]_k A_{k,T_{(l,m)}} T^4_{(l,m)} - [S_{2,i}V_{(l,m)}]_k A_{k,T_{S_{2,i}}} T^4_{S_{2,i}}\right\}\right\}. \tag{4}$$

And $q^r_{S_{2,i}\to S_\infty}$ means the net radiative heat energy that $S_{2,i}$ transfers to S_∞

$$q^r_{S_{2,i}\to S_\infty} = \sigma T^4_{S_{2,i}}\Delta x - C_{S_{2,i}}, \tag{5a}$$

$$C_{S_{2,i}} = \frac{2\sigma T^4_{\infty 1}}{\pi}\int_0^{L_2} dx\int_0^{\pi/2} d\varphi\int_{\arctg\left[\frac{L_2-x}{(i\Delta x-\Delta x+L_1)\cos\varphi}\right]}^{\arctg\left[\frac{L_2-x}{(i\Delta x+L_1)\cos\varphi}\right]}\cos\theta\sin\theta d\theta$$
$$+\frac{2\sigma T^4_{\infty 3}}{\pi}\int_0^{L_2} dx\int_0^{\pi/2} d\varphi\int_{\arctg\left[\frac{L_2-x}{(H_x-i\Delta x+L_3)\cos\varphi}\right]}^{\arctg\left[\frac{L_2-x}{(H_x-(i-1)\Delta x+L_3)\cos\varphi}\right]}\cos\theta\sin\theta d\theta$$
$$+\frac{2\sigma T^4_{\infty 2}}{\pi}\left(\int_0^{L_1+(i-1)\Delta x} dx\int_0^{\pi/2} d\varphi\int_{\arctg\left(\frac{x}{L_2\cos\varphi}\right)}^{\arctg\left(\frac{x+\Delta x}{L_2\cos\varphi}\right)}\cos\theta\sin\theta d\theta\right.$$
$$+\int_0^{L_3+H_x-i\Delta x} dx\int_0^{\pi/2} d\varphi\int_{\arctg\left(\frac{x}{L_2\cos\varphi}\right)}^{\arctg\left(\frac{x+\Delta x}{L_2\cos\varphi}\right)}\cos\theta\sin\theta d\theta$$
$$\left.+2\int_0^{\Delta x} dx\int_0^{\pi/2} d\varphi\int_0^{\arctg\left(\frac{x}{L_2\cos\varphi}\right)}\cos\theta\sin\theta d\theta\right), \tag{5b}$$

where, the term $\sigma T^4_{S_{2,i}}\Delta x$ means the radiative energy that $S_{2,i}$ transfers to S_∞, while $C_{S_{2,i}}$ is a constant, which means the radiative energy that the black surroundings ($S_{\infty 1}$, $S_{\infty 2}$ and $S_{\infty 3}$) transfer to $S_{2,i}$. For simplicity, the deduction of Eq. (5b) is omitted.

3. Solve the RTCs of isotropic scattering media

The solving of isotropic scattering RTCs mainly contains four steps. Firstly, the RTCs without considering scattering must be solved. Secondly, the RTCs solved in the first step are normalized according to their integrality relationships. Thirdly, the normalized RTCs are used to trace the scattering energy to solve the normalized isotropic scattering RTCs. Finally, inverse calculation is carried out to solve the isotropic RTCs of the media.

3.1. Solve the RTCs without considering scattering

Before solving the RTCs for isotropic scattering media, the RTCs without considering scattering must be solved first. In this step the radiative intensity attenuates in accordance with the Bouguer Law, $Ie^{-\kappa_k l}$, where $\kappa_k = \alpha_k + \sigma_k$, I is the radiative intensity, and l is the distance that the radiative intensity passes through the media. The RTCs without considering scattering are expressed by $(V_{(l,m)}V_{(i,j)})_k$, $(S_{1,m}V_{(i,j)})_k$ and $(V_{(i,j)}S_{2,l})_k$, etc. Now we take $(V_{(i,j)}S_{2,l})_k$ as an example to illustrate the deduction of these RTCs, and for simplicity the subscript k is omitted in the following deduction. The RTC $(V_{(i,j)}S_{2,l})_k$ can be expressed as

$$(V_{(i,j)}S_{2,l}) = \sum_{n=1}^{4} f^n_{ij\to S_{2,l}} - \sum_{l'=1}^{4} = f^{n'}_{ij\to S_{2,l}}, \tag{6}$$

where $f^n_{ij\to S_{2,l}}$ means the part of the radiative energy emitted by the outside of interface n of $V_{(i,j)}$ over the whole hemispherical sphere and absorbed by $S_{2,l}$. The superscript n represents the outside of interface n, where n = 1–4, as shown in Fig. 1(b). $f^{n'}_{ij\to S_{2,l}}$ means the part of the radiative energy emitted by the inside of interface n of $V_{(i,j)}$ over the whole hemispherical sphere and absorbed by $S_{2,l}$. The superscript n' denotes the inside of interface n, as shown in Fig. 1(b).

When $S_{2,l}$ is located in the top-right direction of $V_{(i,j)}$, i.e., $l > i$ and $j < N$, the following expressions can be deduced

$$f^2_{ij\to S_{2,l}} = 2\int_{(i-1)\Delta x}^{i\Delta x} dx\int_0^{\frac{\pi}{2}} d\varphi\int_{\arctg\left(\frac{(i-1)\Delta x-x}{(N-j)\Delta y\cos\varphi}\right)}^{\arctg\left(\frac{i\Delta x-x}{(N-j)\Delta y\cos\varphi}\right)}$$
$$\times\exp\left[-\frac{(N-j)\Delta y\kappa}{\cos\theta}\right]\cos\theta\sin\theta d\theta, \tag{7a}$$

$$f^3_{ij\to S_{2,l}}=\begin{cases}2\int_{(j-1)\Delta y}^{j\Delta y}dy\int_0^{\frac{\pi}{2}}d\varphi\int_{\operatorname{arctg}\left(\frac{H_y-y}{(l-1-i)\Delta x\cos\varphi}\right)}^{\frac{\pi}{2}}\exp\left[-\frac{(H_y-y)K}{\sin\theta\cos\varphi}\right]\cos\theta\sin\theta d\theta\quad(l\neq i+1),\\ 2\int_{(j-1)\Delta y}^{j\Delta y}dy\int_0^{\frac{\pi}{2}}d\varphi\int_{\operatorname{arctg}\left(\frac{H_y-y}{(l-i)\Delta x\cos\varphi}\right)}^{\frac{\pi}{2}}\exp\left[-\frac{(H_y-y)K}{\sin\theta\cos\varphi}\right]\cos\theta\sin\theta d\theta\quad(l=i+1),\end{cases}\tag{7b}$$

$$f^1_{ij\to S_{2,l}}=f^4_{ij\to S_{2,l}}=0.\tag{7c}$$

We can refer to Ref. [29] to get more information about the deduction of Eq. (7). Moreover, $f^{n'}_{ij\to S_{2,l}}$ can be simply deduced from Eq. (7)

$$\begin{aligned}&f^{2'}_{ij\to S_{2,l}}=f^4_{i(j+1)\to S_{2,l}},\quad f^{1'}_{ij\to S_{2,l}}=f^3_{(i-1)j\to S_{2,l}},\\&f^{3'}_{ij\to S_{2,l}}=f_{(i+1)j\to S^1_{2,l}},\quad f^{4'}_{ij\to S_{2,l}}=f_{i(j-1)\to S^2_{2,l}}.\end{aligned}\tag{8}$$

Then, the RTC $(V_{(i,j)}S_{2,l})$ can be calculated by substitution of Eqs. (7) and (8) into Eq. (6).

3.2. Reciprocity and integrality relationships of RTCs without considering scattering

The RTCs without considering scattering have reciprocity relationships and integrality relationships. The reciprocity relationships are given by Eq. (9), while the integrality relationships are given by the Eq. (10). On the one hand, these relationships are used to validate the correctness of the RTCs, and on the other hand, the integrality relationships, Eq. (10), are used to normalize the RTCs without considering scattering before solving the RTCs of isotropic scattering media.

$$\begin{aligned}&(S_{1,j}S_{2,i})_k=(S_{2,i}S_{1,j})_k,\quad(S_{1,j}S_{3,j})_k=(S_{3,j}S_{1,j})_k,\quad(S_{1,j}S_{4,i})_k=(S_{4,i}S_{1,j})_k,\\&(S_{2,i}S_{3,j})_k=(S_{3,j}S_{2,i})_k,\quad(S_{2,i}S_{4,l})_k=(S_{4,l}S_{2,i})_k,\quad(S_{3,j}S_{4,i})_k=(S_{4,i}S_{3,j})_k,\\&(S_{1,j}V_{(i,j)})_k=(V_{(i,j)}S_{1,j})_k,\quad(S_{2,i}V_{(i,j)})_k=(V_{(i,j)}S_{2,i})_k,\\&(S_{3,j}V_{(i,j)})_k=(V_{(i,j)}S_{3,j})_k,\quad(S_{4,i}V_{(i,j)})_k=(V_{(i,j)}S_{4,i})_k,\\&(V_{(i,j)}V_{(l,m)})_k=(V_{(l,m)}V_{(i,j)})_k.\end{aligned}\tag{9}$$

$$\begin{aligned}&\sum_{l=1}^{M}\sum_{m=1}^{N}(V_{(i,j)}V_{(l,m)})_k+\sum_{j=1}^{N}\left[(V_{(i,j)}S_{1,j})_k+(V_{(i,j)}S_{3,j})_k\right]\\&\quad+\sum_{i=1}^{M}\left[(V_{(i,j)}S_{2,i})_k+(V_{(i,j)}S_{4,i})_k\right]=4\pi\alpha_k\Delta x\Delta y,\\&\sum_{l=1}^{M}\sum_{m=1}^{N}(S_{1,j}V_{(l,m)})_k+\sum_{i=1}^{M}\left[(S_{1,j}S_{2,i})_k+(S_{1,j}S_{4,i})_k\right]+\sum_{J=1}^{N}(S_{1,j}S_{3,J})_k=\pi\Delta y,\\&\sum_{l=1}^{M}\sum_{m=1}^{N}(S_{3,j}V_{(l,m)})_k+\sum_{i=1}^{M}\left[(S_{3,j}S_{2,i})_k+(S_{3,j}S_{4,i})_k\right]+\sum_{J=1}^{N}(S_{3,j}S_{1,J})_k=\pi\Delta y,\\&\sum_{l=1}^{M}\sum_{m=1}^{N}(S_{2,i}V_{(l,m)})_k+\sum_{j=1}^{N}\left[(S_{2,i}S_{1,j})_k+(S_{2,i}S_{3,j})_k\right]+\sum_{I=1}^{M}(S_{2,i}S_{4,I})_k=\pi\Delta x,\\&\sum_{l=1}^{M}\sum_{m=1}^{N}(S_{4,i}V_{(l,m)})_k+\sum_{j=1}^{N}\left[(S_{4,i}S_{1,j})_k+(S_{4,i}S_{3,j})_k\right]+\sum_{I=1}^{M}(S_{4,i}S_{2,I})_k=\pi\Delta x.\end{aligned}\tag{10}$$

3.3. Solve the RTCs of isotropic scattering media

3.3.1. Normalization of the RTCs without considering scattering

For absorbing, isotropically scattering media, part of the radiative energy represented by RTC $(V_{(i,j)}V_{(l,m)})_k$, etc., is absorbed, and the rest is scattered. The following process should be carried out. Because the following deduction implies a precondition that the energy redistributed must be unity, the RTCs of the absorbing media should be normalized initially, according to Eq. (10). That is

$$\begin{aligned}&(V_{(i,j)}V_{(l,m)})^*_k=(V_{(i,j)}V_{(l,m)})_k/(4\alpha_k\Delta x\Delta y)\quad(i,l=1{-}M,\text{ and }j,m=1{-}N),\\&(V_{(i,j)}S_{u,m})^*_k=(V_{(i,j)}S_{u,m})_k/(4\alpha_k\Delta x\Delta y)\quad(i=1{-}M,j,m=1{-}N\text{ and }u=1\text{ or }3),\\&(V_{(i,j)}S_{u,m})^*_k=(V_{(i,j)}S_{u,m})_k/(4\alpha_k\Delta x\Delta y)\quad(i,m=1{-}M,j=1{-}N\text{ and }u=2\text{ or }4),\\&(S_{u,m}V_{(i,j)})^*_k=(S_{u,m}V_{(i,j)})_k/(\pi\Delta y)\quad(i=1{-}M,j,m=1{-}N,\text{ and }u=1\text{ or }3),\\&(S_{u,m}V_{(i,j)})^*_k=(S_{u,m}V_{(i,j)})_k/(\pi\Delta x)\quad(i,m=1{-}M,j=1{-}N,\text{ and }u=2\text{ or }4),\\&(S_{1,m}S_{v,l})^*_k=(S_{1,m}S_{v,l})_k/(\pi\Delta y)\quad(l=1{-}M,m=1{-}N,\text{ and }v=2\text{ or }4),\\&(S_{1,m}S_{v,l})^*_k=(S_{1,m}S_{v,l})_k/(\pi\Delta y)\quad(l,m=1{-}N,\text{ and }v=3),\\&(S_{3,m}S_{v,l})^*_k=(S_{3,m}S_{v,l})_k/(\pi\Delta y)\quad(l=1{-}M,m=1{-}N,\text{ and }v=2\text{ or }4),\\&(S_{3,m}S_{v,l})^*_k=(S_{3,m}S_{v,l})_k/(\pi\Delta y)\quad(l,m=1{-}N\text{ and }v=1),\\&(S_{2,m}S_{v,l})^*_k=(S_{2,m}S_{v,l})_k/(\pi\Delta x)\quad(l=1{-}N,m=1{-}M,\text{ and }v=1\text{ or }3),\\&(S_{2,m}S_{v,l})^*_k=(S_{2,m}S_{v,l})_k/(\pi\Delta x)\quad(l,m=1{-}M,\text{ and }v=4),\\&(S_{4,m}S_{v,l})^*_k=(S_{4,m}S_{v,l})_k/(\pi\Delta x)\quad(l=1{-}N,m=1{-}M,\text{ and }v=1\text{ or }3),\\&(S_{4,m}S_{v,l})^*_k=(S_{4,m}S_{v,l})_k/(\pi\Delta x)\quad(l,m=1{-}M,\text{ and }v=2).\end{aligned}\tag{11}$$

where the asterisk denotes normalized RTCs.

3.3.2. Trace the scattering energy to solve the RTCs of isotropic scattering media

As shown in Eq. (2), the isotropic scattering RTCs can be classified into four categories: (1) control volume vs control volume: $[V_{(i,j)}V_{(l,m)}]_k$; (2) control volume vs surface element: $[V_{(i,j)}S_{u,m}]_k$; (3) surface element vs control volume: $[S_{u,m}V_{(i,j)}]_k$; and (4) surface element vs surface element: $[S_{u,m}S_{v,l}]_k$. The deduction of these isotropic RTCs is similar, so, for simplicity take the RTC $[V_{(i,j)}V_{(l,m)}]_k$ as an example to illustrate the deductive process. Define $\eta_k=1-\omega_k$, which means the kth spectral band absorption quotient of the total attenuated energy by a control volume. For convenience, in the following the subscript k is omitted, and subscript a and A are introduced to denote the absorption quotient. Notice that only the medium scatters but the surfaces do not. The isotropic scattering effect can be considered as follows.

(1) After the first tracing event of the scattering energy, the absorbed part of the quotient $(V_{(i,j)}V_{(l,m)})^*$ by $V_{(l,m)}$ is

$$[V_{(i,j)}V_{(l,m)}]^{*1\text{st}}_a=(V_{(i,j)}V_{(l,m)})^*\eta,\tag{12}$$

and the scattering part by $V_{(l,m)}$ is $(V_{(i,j)}V_{(l,m)})^*\omega$.

(2) After the second tracing event of the scattering energy, the energy emitted by $V_{(i,j)}$ and scattered by all control volumes is $\sum_{l_2=1}^{M}\sum_{m_2=1}^{N}(V_{(i,j)}V_{(l_2,m_2)})^*\omega$, which is homogeneously distributed over the whole spherical space and can be considered equivalent to that isotropically emitted by the control volume $V_{(l,m)}$. This scattering tracing event causes the portion

$$[V_{(i,j)}V_{(l,m)}]^{*2\text{nd}}_A=\sum_{l_2=1}^{M}\sum_{m_2=1}^{N}(V_{(i,j)}V_{(l_2,m_2)})^*\omega(V_{(l_2,m_2)}V_{(l,m)})^*\eta,\tag{13}$$

to be absorbed by $V_{(l,m)}$:

$$[V_{(i,j)}V_{(l,m)}]^{*2\text{nd}}_a=[V_{(i,j)}V_{(l,m)}]^{*1\text{st}}_a+[V_{(i,j)}V_{(l,m)}]^{*2\text{nd}}_A,\tag{14}$$

(3) Part $\sum_{l_3=1}^{M}\sum_{m_3=1}^{N}[(V_{(i,j)}V_{(l_3,m_3)})^*\omega\sum_{l_2=1}^{M}\sum_{m_2=1}^{N}(V_{(l_3,m_3)}V_{(l_2,m_2)})^*\omega]$ of the scattered energy $\sum_{l_2=1}^{M}\sum_{m_2=1}^{N}(V_{(i,j)}V_{(l_2,m_2)})^*\omega$, derived in step 2, is scattered again, and this causes some of the radiative energy, emitted by $V_{(i,j)}$, to be absorbed by $V_{(l,m)}$ once more. Thus, the third tracing event of the scattering energy causes the portion

$$[V_{(i,j)}V_{(l,m)}]^{*3\text{rd}}_A=\sum_{l_3=1}^{M}\sum_{m_3=1}^{N}\left[\left(V_{(i,j)}V_{(l_3,m_3)}\right)^*\omega\sum_{l_2=1}^{M}\sum_{m_2=1}^{N}\left(V_{(l_3,m_3)}V_{(l_2,m_2)}\right)^*\times\omega(V_{(l_2,m_2)}V_{(l,m)})^*\eta\right],\tag{15a}$$

to be absorbed by $V_{(l,m)}$. Eq. (15a) can be written as

$$[V_{(i,j)}V_{(l,m)}]^{*3\text{rd}}_A=\sum_{l_3=1}^{M}\sum_{m_3=1}^{N}\left[\left(V_{(i,j)}V_{(l_3,m_3)}\right)^*\omega[V_{(l_3,m_3)}V_{(l,m)}]^{*2\text{nd}}_A\right],\tag{15b}$$

where $[V_{(l_3,m_3)}V_{(l,m)}]_A^{*2nd}$ can be calculated form Eq. (13) by replacing $V_{(i,j)}$ with $V_{(l_3,m_3)}$. So, after the third tracing event of the scattering energy, we have

$$[V_{(i,j)}V_{(l,m)}]_a^{*3rd} = [V_{(i,j)}V_{(l,m)}]_a^{*2nd} + [V_{(i,j)}V_{(l,m)}]_A^{*3rd}. \quad (16)$$

(4) The scattered energy $\sum_{l_3=1}^{M}\sum_{m_3=1}^{N}[(V_{(i,j)}V_{(l_3,m_3)})^*\omega\sum_{l_2=1}^{M}\sum_{m_2=1}^{N}(V_{(l_3,m_3)}V_{(l_2,m_2)})^*\omega]$, derived in step 3, will be scattered again, and this causes part of the radiative energy to be absorbed by $V_{(l,m)}$ for the fourth tracing event of the scattering energy. Thus, trace the scattered energy repeatedly in this way.

(5) As the number of tracing event increases, the quotient of the scattering energy decreases. So, after the nth tracing event of the scattering energy, if all of the control volumes satisfy the following inequality:

$$\left|1-\sum_{m=1}^{N}\left\{[V_{(i,j)}S_{1,m}]_a^{*nth}+[V_{(i,j)}S_{3,m}]_a^{*nth}\right\}-\sum_{l=1}^{M}\left\{[V_{(i,j)}S_{2,l}]_a^{*nth}+[V_{(i,j)}S_{4,l}]_a^{*nth}\right\}-\sum_{l=1}^{M}\sum_{m=1}^{N}[V_{(i,j)}V_{(l,m)}]_a^{*nth}\right|<10^{-10}, \quad (17)$$

the calculation is finished. And then, we have

$$[V_{(i,j)}V_{(l,m)}]_a^{*nth} = [V_{(i,j)}V_{(l,m)}]_a^{*(n-1)th} + [V_{(i,j)}V_{(l,m)}]_A^{*nth}, \quad (18a)$$

where

$$[V_{(i,j)}V_{(l,m)}]_A^{*nth} = \sum_{l_n=1}^{M}\sum_{m_n=1}^{N}\left[(V_{(i,j)}V_{(l_n,m_n)})^*\omega[V_{(l_n,m_n)}V_{(l,m)}]_A^{*(n-1)th}\right]. \quad (18b)$$

From Eq. (18b) we can see that, $[V_{(i,j)}V_{(l,m)}]_A^{*nth}$ can be calculated through iteration.

Then, $[V_{(i,j)}V_{(l,m)}]$ can be calculated from the inverse calculation:

$$[V_{(i,j)}V_{(l,m)}] = 4\kappa\eta\Delta x\Delta y[V_{(i,j)}V_{(l,m)}]_a^{*nth}. \quad (19)$$

The above deductive process is similar to that of Ref. [24]. The deduction of the other three categories of isotropic scattering RTC is shown in Appendix A.

4. Numerical method and validation of this paper

4.1. Numerical method

As shown in Eqs. (2)–(5), the RST and opaque boundary condition are non-linear functions of temperatures of all nodes, respectively, thus, the Patankar's linearization method is used to linearize the RST and opaque boundary condition. The RST can be linearized as [23–30]

$$\Phi_{(i,j)}^{r,n+1} = Sc_{(i,j)}^{n+1} + Sp_{(i,j)}^{n+1}\cdot T_{(i,j)}^{n+1}, \quad (20)$$

where $Sp_{(i,j)}^{n+1} = (d\Phi_{(i,j)}^{r}/dT_{(i,j)})^n$, $Sc_{(i,j)}^{n+1} = \Phi_{(i,j)}^{r,n} - (d\Phi_{(i,j)}^{r}/dT_{(i,j)})^n\cdot T_{(i,j)}^{n}$. Superscript $(n+1)$ means the $(n+1)$th iterative calculation.

Eq. (1) can be rewritten as the following form:

$$A_{(i,j)}T_{(i,j)}^{m+1} = B_{(i,j)}T_{(i+1,j)}^{m+1} + C_{(i,j)}T_{(i-1,j)}^{m+1} + D_{(i,j)}T_{(i,j+1)}^{m+1} + E_{(i,j)}T_{(i,j-1)}^{m+1} + F_{(i,j)}, \quad (21)$$

where $A_{(i,j)}$, $B_{(i,j)}$, $C_{(i,j)}$, $D_{(i,j)}$, $E_{(i,j)}$ and $F_{(i,j)}$ are the coefficients related to Eq. (1). The alternating direction implicit (ADI) method is used to solve the linearized equations. The principle of ADI method is that, when solving along one direction, the variables along this direction are implicit, and the variables along the other directions are explicit. Scan line by line along vertical direction over the full rectangular region at first, and then scan row by row along horizontal direction, and the two scanning steps compose one round iteration [31]. We can refer to Ref. [32] to get more information about the numerical method.

4.2. Validation of this paper

Using the Lattice Boltzmann method to solve the energy equation and the finite volume method to calculate the RST, Mishra et al. [8] studied transient coupled heat transfer in a rectangular medium with imposed boundary temperatures. The calculating parameters are $L_r = 1$ m, $H_x^* = H_y^* = 1$, $n = 1$, and $\kappa = 1\ \mathrm{m}^{-1}$, $T_0 = T_{g1} = T_{g2} = T_{g3} = T_{g4}/2$, $T_r = T_{g4}$, $h_1 = h_2 = h_3 = h_4 = 10^{10}\ \mathrm{W\,m^{-2}\,K^{-1}}$ (infinitely large). The medium is gray ($NB = 1$). In Ref. [8], the dimensionless time is defined as $\xi_i = \alpha\kappa^2 t_i$, where $\alpha(=k/(\rho c))$ is the thermal diffusivity, and the conduction-radiation parameter is defined as $N' = k\kappa/(4\sigma T_r^3)$. The number of control volume is taken as $M = N = 25$. The dimensionless time intervals are $\Delta\xi_1 = 0.003$, $\Delta\xi_2 = 0.0008$ and $\Delta\xi_3 = 10$.

In this case, suppose that the temperature fields reach the steady state when the temperatures of all nodes between the mth time increment and the $(m+1)$th one satisfy $|T_{(i,j)}^{m+1} - T_{(i,j)}^{m}| < 10^{-7}$. Corresponding to the mth time increment, if the temperatures of all nodes between the nth iteration calculation and the $(n+1)$th one satisfy $|T_{(i,j)}^{m,n+1} - T_{(i,j)}^{m,n}| < 10^{-5}$, the convergent results are reached.

Because the convective coefficients are infinitely large, the temperatures at the four sides of the rectangular medium are kept unchanged in the transients, equal to the temperatures of their surrounding fluids. The results are shown in Fig. 2, in which we can see that the results of this paper agree very well with those of Mishra's [8]. This partially proves that the RTCs of absorbing media, the RTCs of isotropic scattering media, and the numerical method of this paper are correct.

5. Results and discussion

The calculating parameters of Fig. 3 are $\omega = 0.98$, $L_r = 1.0$ m, $N = 0.1$, $n = 2.2$, $\kappa = 1\ \mathrm{m}^{-1}$, $H_x^* = H_y^* = 1.5$, $M = N = 55$, $T_0 = T_r =$

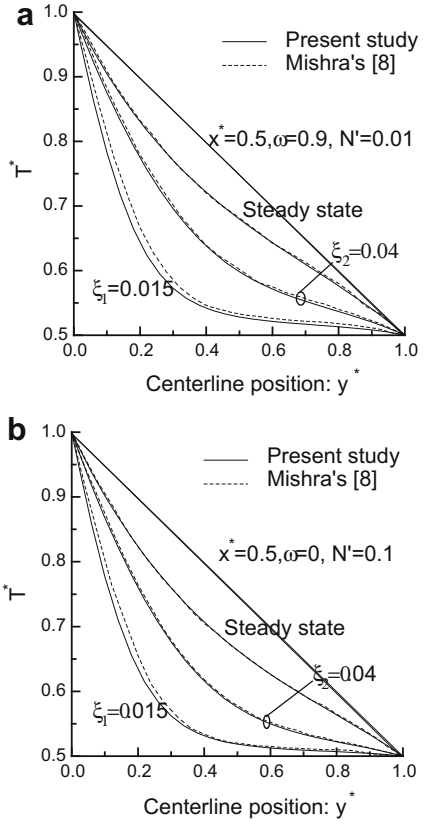

Fig. 2. Comparison with Mishra's results. (a) $\omega = 0.9, N' = 0.01$; and (b) $\omega = 0, N' = 0.1$.

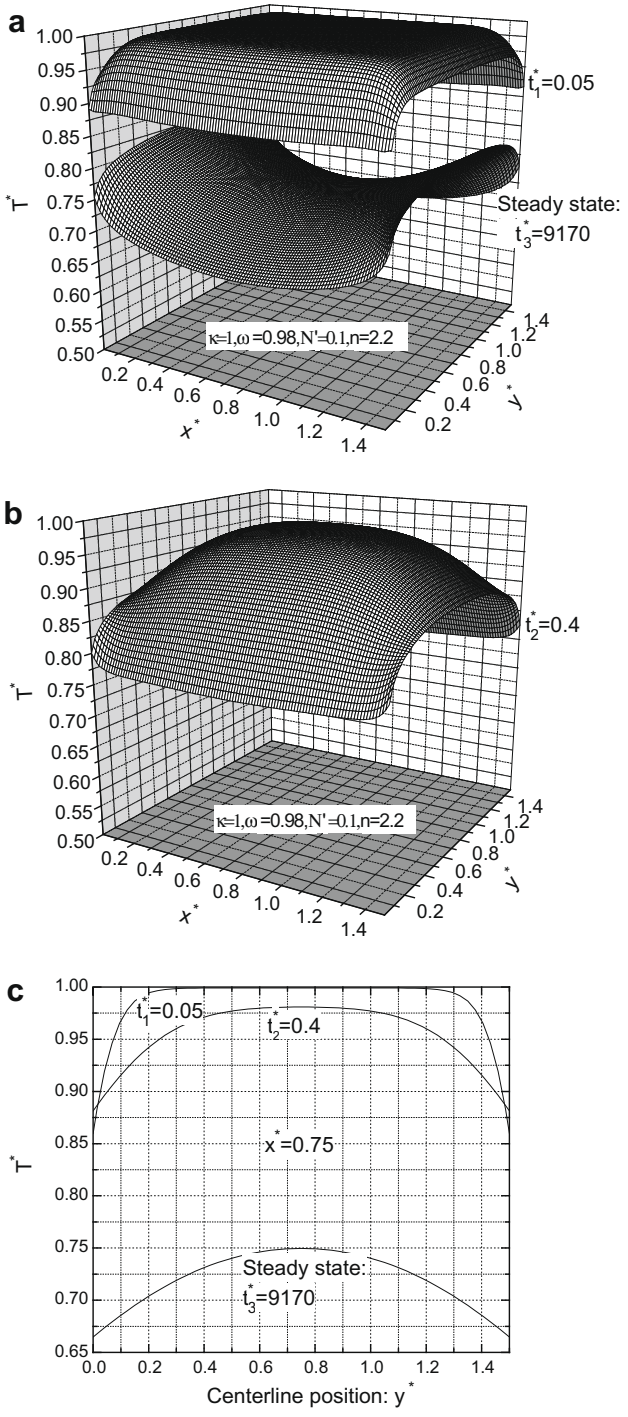

Fig. 3. Temperature distribution for the basic parameters. (a) $t_1^* = 0.05$ and steady state; (b) $t_1^* = 0.4$; and (c) temperature distribution along the vertical centerline position.

1000 K, $h_1 = h_2 = h_3 = h_4 = 100\ \mathrm{W\,m^{-2}\,K^{-1}}$, $T_{\infty 1} = T_{g1} = T_{\infty 3} = T_{g3} =$ 1000 K, $L_1^* = L_2^* = L_3^* = L_4^* = 1.0$, $T_{\infty 2} = T_{g2} = T_{\infty 4} = T_{g4} = 300$ K. The medium is gray ($NB = 1$), and the time intervals are $\Delta t_1^* = 0.01, \Delta t_2^* = 0.008$ and $\Delta t_3^* = 10$. The steady state to be defined when the temperatures of all nodes between the mth time increment and the $(m+1)$th one satisfy $|T_{(i,j)}^{m+1} - T_{(i,j)}^{m}| < 10^{-7}$. Corresponding to the mth time increment, if the temperatures of all nodes between the nth iteration calculation and the $(n+1)$th one satisfy $|T_{(i,j)}^{m,n+1} - T_{(i,j)}^{m,n}| < 10^{-5}$, the convergent solution is reached.

As shown in Fig. 3, during the transient beginning, although S_1 and S_3 are heated by their surroundings, they are cooled more quickly than the central medium because they can intensively transfer radiative energy passing through the inner media to S_2 and S_4, which are of lower temperature, for the reasons that the media are strongly scattering and weakly absorbing. The temperature profile is concave downwards during the transient beginning and like a saddle of horse at steady state.

Keeping the other parameters of Fig. 3 unchanged, effect of $\omega = 0.5$ on temperature distribution is shown in Fig. 4. When the scattering albedo decreases, the absorption coefficient increases and the emitting ability of the media is intensified. So, compared with Fig. 3, it can be seen that, the cooling effect of the central media is intensified, and as a result, the temperatures of the central media decrease during the transient beginning, and at the same time, the temperatures of S_2 and S_4 increase because they receive more radiative energy emitted from the central media. The time to reach steady state is also much reduced.

Keeping the other parameters of Fig. 3 unchanged, effect of $n = 4.2$ on temperature distribution is shown in Fig. 5. Due to reason that the emitting ability of medium is proportional to the square of refractive index, the emitting ability of medium is intensified when refractive index of the medium increases. Thus, compared with Fig. 3, we can see that, the saddle shape of the temperature profile at steady state becomes unconspicuous, and the temperatures distribute more homogeneous within the media. The time to reach steady state is reduced.

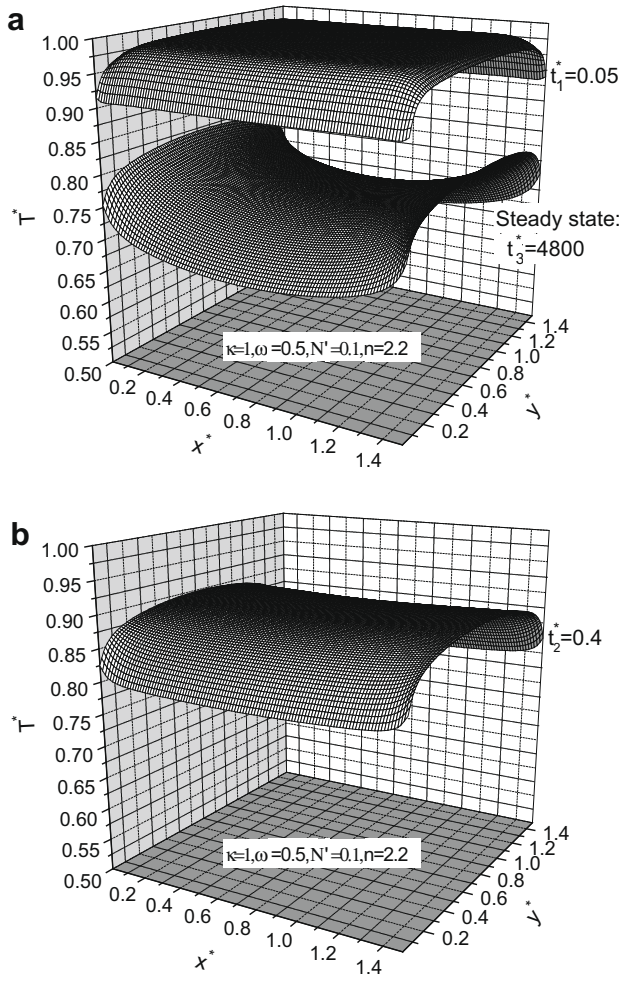

Fig. 4. Effect of scattering albedo on temperature distribution. (a) $t_1^* = 0.05$ and steady state; (b) $t_1^* = 0.4$.

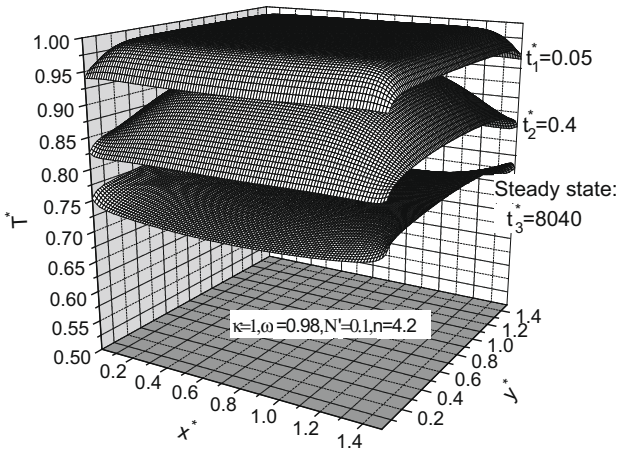

Fig. 5. Effect of refractive index on temperature distribution.

6. Conclusions

In this paper the RTNAM is extended to solve the 2-D transient coupled heat transfer in a rectangular isotropic scattering medium. Before solving the RTCs of isotropic scattering medium, the RTCs without considering scattering must be solved at first. Then the RTCs without considering scattering are normalized according to their integrality relationships. The normalized RTCs are used to trace the scattering energy. It is found that the energy quotient of the nth tracing event of the scattering energy can be calculated from that of the $(n-1)$th tracing event. This makes the RTCs of isotropic scattering medium can be calculated by iteration. The correctness of this paper is validated. Effects of ω and n on temperature distribution are investigated, and for simplicity, effects of the other parameters, such as κ, N, $T_{\infty i}$ (i = 1–4), h_i and L_i, etc., on temperature distribution are neglected.

Our study shows that the RTNAM can provide very accurate results and has a good convergent property, although the deductive process of the RTCs is very complex. The computer we use to calculate the results is a Dell PowerEdge 2900 Server, 1.6 GHz dual-core processors with 8 GB RAM, which is installed with Linux operating system and Intel Fortran compiler. With this computer, it takes about several hours to calculate one group of results in one figure. We think that this time consumption can be accepted.

Acknowledgments

This research is supported by the Foundation for the Author of National Excellent Doctoral Dissertation of PR China (Grant 200438) and supported by the National Natural Science Foundation of PR China (Project 50806018).

Appendix A. Deduction of the RTCs of isotropic scattering medium

The RTC $[V_{(i,j)}V_{(l,m)}]_k$ is detailedly solved in the text, and the solving of the other RTCs is similar to that. So, for simplicity we only give the final results here. After the nth tracing event of the scattering energy, we have

$$(1)\qquad [V_{(i,j)}S_{u,m}] = 4\kappa\eta\Delta x\Delta y[V_{(i,j)}S_{u,m}]_a^{*n\text{th}} \quad (u = 1-4)$$

where, $[V_{(i,j)}S_{u,m}]_a^{*n\text{th}} = [V_{(i,j)}S_{u,m}]_a^{*(n-1)\text{th}} + [V_{(i,j)}S_{u,m}]_A^{*n\text{th}}$, $[V_{(i,j)}S_{u,m}]_A^{*n\text{th}} = \sum_{l_n=1}^{M}\sum_{m_n=1}^{N}\left[(V_{(i,j)}V_{(l_n,m_n)})^*\omega[V_{(l_n,m_n)}S_{u,m}]_A^{*(n-1)\text{th}}\right]$, $[V_{(i,j)}S_{u,m}]_a^{*1\text{st}} = (V_{(i,j)}S_{u,m})^*$, and $[V_{(i,j)}S_{u,m}]_A^{*2\text{nd}} = \sum_{l_2=1}^{M}\sum_{m_2=1}^{N}[(V_{(i,j)}V_{(l_2,m_2)})^*\omega(V_{(l_2,m_2)}S_{u,m})^*]$.

$$(2)\qquad [S_{u,m}V_{(i,j)}] = \begin{cases} \pi\Delta y[S_{u,m}V_{(i,j)}]_a^{*n\text{th}} & (u = 1,3) \\ \pi\Delta x[S_{u,m}V_{(i,j)}]_a^{*n\text{th}} & (u = 2,4) \end{cases}$$

where, $[S_{u,m}V_{(i,j)}]_a^{*1\text{st}} = (S_{u,m}V_{(i,j)})^*\eta$, $[S_{u,m}V_{(i,j)}]_a^{*2\text{nd}} = [S_{u,m}V_{(i,j)}]_a^{*1\text{st}} + \sum_{l_2=1}^{M}\sum_{m_2=1}^{N}[(S_{u,m}V_{(l_2,m_2)})^*\omega(V_{(l_2,m_2)}V_{(i,j)})^*\eta]$, $[S_{u,m}V_{(i,j)}]_a^{*3\text{rd}} = [S_{u,m}V_{(i,j)}]_a^{*2\text{nd}} + \sum_{l_3=1}^{M}\sum_{m_3=1}^{N}\left[(S_{u,m}V_{(l_3,m_3)})^*\omega[V_{(l_3,m_3)}V_{(i,j)}]_A^{*3\text{rd}}\right]$, and $[V_{(l_3,m_3)}V_{(i,j)}]_A^{3\text{rd}} = \sum_{l_2=1}^{M}\sum_{m_2=1}^{N}(V_{(l_3,m_3)}V_{(l_2,m_2)})^*\omega(V_{(l_2,m_2)}V_{(i,j)})^*\eta$. If $n \geqslant 4$, then $[S_{u,m}V_{(i,j)}]_a^{*n\text{th}} = [S_{u,m}V_{(i,j)}]_a^{*(n-1)\text{th}} + [S_{u,m}V_{(i,j)}]_A^{*n\text{th}}$, where, $[S_{u,m}V_{(i,j)}]_A^{*n\text{th}} = \sum_{l_n=1}^{M}\sum_{m_n=1}^{N}\left[(S_{u,m}V_{(l_n,m_n)})^*\omega[V_{(l_n,m_n)}V_{(i,j)}]_A^{*n\text{th}}\right]$, and $[V_{(l_n,m_n)}V_{(i,j)}]_A^{*n\text{th}} = \sum_{l_{n-1}=1}^{M}\sum_{m_{n-1}=1}^{N}[(V_{(l_n,m_n)}V_{(l_{n-1},m_{n-1})})^*\omega[V_{(l_{n-1},\ m_{n-1})}V_{(i,j)}]_A^{*(n-1)\text{th}}]$.

$$(3)\qquad [S_{u,m}S_{v,l}] = \begin{cases} \pi\Delta y[S_{u,m}S_{v,l}]_a^{*n\text{th}} & (u = 1,3) \\ \pi\Delta x[S_{u,m}S_{v,l}]_a^{*n\text{th}} & (u = 2,4) \end{cases}$$

where, $[S_{u,m}S_{v,l}]_a^{*1\text{st}} = \begin{cases} (S_{u,m}S_{v,l})^* & (v \neq u) \\ 0 & (v = u) \end{cases}$, $[S_{u,m}S_{v,l}]_a^{*2\text{nd}} = [S_{u,m}S_{v,l}]_a^{*1\text{st}} + \sum_{l_2=1}^{M}\sum_{m_2=1}^{N}[(S_{u,m}V_{(l_2,m_2)})^*\omega(V_{(l_2,m_2)}S_{v,l})^*]$, $[S_{u,m}S_{v,l}]_a^{*3\text{rd}} = [S_{u,m}S_{v,l}]_a^{*2\text{nd}} + \sum_{l_3=1}^{M}\sum_{m_3=1}^{N}\left[(S_{u,m}V_{(l_3,m_3)})^*\omega[V_{(l_3,m_3)}S_{v,l}]_A^{*3\text{rd}}\right]$, and $[V_{(l_3,m_3)}S_{v,l}]_A^{3\text{rd}} = \sum_{l_2=1}^{M}\sum_{m_2=1}^{N}(V_{(l_3,m_3)}V_{(l_2,m_2)})^*\omega(V_{(l_2,\ m_2)}S_{v,l})^*$. If $n \geqslant 4$, then $[S_{u,m}V_{(i,j)}]_a^{*n\text{th}} = [S_{u,m}S_{v,l}]_a^{*(n-1)\text{th}} + [S_{u,m}S_{v,l}]_A^{*n\text{th}}$, where, $[S_{u,m}S_{v,l}]_A^{*n\text{th}} = \sum_{l_n=1}^{M}\sum_{m_n=1}^{N}\left[(S_{u,m}V_{(l_n,m_n)})^*\omega[V_{(l_n,m_n)}S_{v,l}]_A^{*n\text{th}}\right]$, and $[V_{(l_n,m_n)}S_{v,l}]_A^{*n\text{th}} = \sum_{l_{n-1}=1}^{M}\sum_{m_{n-1}=1}^{N}[(V_{(l_n,m_n)}V_{(l_{n-1},m_{n-1})})^*\omega[V_{(l_{n-1},m_{n-1})}\ S_{v,l}]_A^{*(n-1)\text{th}}]$.

References

[1] R. Siegel, Radiative exchange in a parallel-plate enclosure with translucent protective coatings on its walls, Int. J. Heat Mass Transfer 42 (1998) 73–84.
[2] K.H. Lee, R. Viskanta, Comparison of the diffusion approximation and the discrete ordinates method for the investigation of heat transfer in glass, Glass Sci. Technol. – Glastechnische Berichte 72 (1999) 254–265.
[3] J.L. Cordova, A.C. Fernandez-Pello, Convection effects on the endothermic gasification and piloted ignition of a radiatively heated combustible solid, Combust. Sci. Technol. 156 (2000) 271–289.
[4] J.F. Luo, H.L. Yi, H.P. Tan, L.J. Yang, Thermal analysis of optical windows for spacecraft application, J. Thermophys. Heat Transfer 22 (2) (2008) 296–301.
[5] S.C. Mishra, P. Talukdar, D. Trimis, F. Durst, Computational efficiency improvements of the radiative transfer problems with or without conduction – a comparison of the collapsed dimension method and the discrete transfer method, Int. J. Heat Mass Transfer 46 (2003) 3083–3095.
[6] S.C. Mishra, A. Lankadasu, K.N. Beronov, Application of the Lattice Boltzmann method for solving the energy equation of a 2-D transient conduction-radiation problem, Int. J. Heat Mass Transfer 48 (2005) 3648–3659.
[7] S.C. Mishra, P. Talukdar, D. Trimis, F. Durst, Two-dimensional transient conduction and radiation heat transfer with temperature dependent thermal conductivity, Int. Commun. Heat Mass Transfer 32 (2005) 305–314.
[8] S.C. Mishra, H.K. Roy, Solving transient conduction and radiation heat transfer problems using the Lattice Boltzmann method and the finite volume method, J. Comput. Phys. 223 (2007) 89–107.
[9] P. Furmanski, J. Banaszek, Finite element analysis of concurrent radiation and conduction in participating media, J. Quant. Spectrosc. Radiat. Transfer 84 (2004) 563–573.
[10] T.Y. Kim, S.W. Baek, Analysis of combined conductive and radiative heat transfer in a two-dimensional rectangular enclosure using the discrete ordinate method, Int. J. Heat Mass Transfer 34 (1991) 2265–2273.
[11] R. Viskanta, K.H. Lee, Two-dimensional combined conduction and radiation heat transfer: comparison of the discrete ordinate method and the diffusion approximation methods, Numer. Heat Transfer Part A 39 (2001) 205–225.
[12] D. Lacroix, G. Parent, F. Asllanaj, G. Jeandel, Coupled radiative and conductive heat transfer in a non-grey absorbing and emitting semitransparent media under collimated radiation, J. Quant. Spectrosc. Radiat. Transfer 75 (2002) 589–609.
[13] S.K. Mahapatra, S.B. Mahapatra, Numerical modeling of combined conductive and radiative heat transfer within square enclosure using discrete ordinate method, Heat Mass Transfer 40 (2004) 533–538.

[14] D. Lacroix, N. Berour, P. Boulet, G. Jeandel, Transient radiative and conductive heat transfer in non-gray semitransparent two dimensional media with mixed boundary conditions, Heat Mass Transfer 42 (2006) 322–337.
[15] C.Y. Wu, S.H. Wu, Integral equation formulation for transient radiative transfer in an anisotropically scattering medium, Int. J. Heat Mass Transfer 43 (2000) 2009–2020.
[16] S.H. Wu, C.Y. Wu, Integral equation solution for transient radiative transfer in nonhomogeneous anisotropically scattering media, J. Heat Transfer 122 (2000) 818–822.
[17] L.H. Liu, H.P. Tan, Transient radiation and conduction in a two dimensional participating cylinder subjected to a pulse irradiation, Int. J. Therm. Sci. 40 (2001) 877–889.
[18] R. Vaillon, M. Lallemand, D. Lemonnier, Radiative heat transfer in orthogonal curvilinear coordinates using the discrete ordinates method, J. Quant. Spectrosc. Radiat. Transfer 55 (1996) 7–17.
[19] V. Feldheim, P. Lybaert, Solution of radiative heat transfer problem with discrete transfer method applied to triangular meshes, J. Comput. Appl. Math. 168 (2004) 179–190.
[20] F. Asllanaj, V. Feldheim, P. Lybaert, Solution of radiative heat transfer in 2-D geometries by a modified finite-volume method based on a cell vertex scheme using unstructured triangular meshes, Numer. Heat Transfer Part B 51 (2007) 97–119.
[21] F. Asllanaj, G. Parent, G. Jeandel, Transient radiation and conduction heat transfer in a gray absorbing-emitting medium applied on two-dimensional complex-shaped domains, Numer. Heat Transfer Part B 52 (2007) 179–200.
[22] M. Sakami, A. Charette, V.L. Dez, Application of the discrete ordinates method to combined conductive and radiative heat transfer in a two-dimensional complex, J. Quant. Spectrosc. Radiat. Transfer 56 (1996) 513–517.
[23] H.P. Tan, M. Lallemand, Transient radiative–conductive heat transfer in flat glasses submitted to temperature, flux and mixed boundary conditions, Int. J. Heat Mass Transfer 32 (1989) 795–810.
[24] H.P. Tan, L.M. Ruan, X.L. Xia, Q.Z. Yu, T.W. Tong, Transient coupled radiative and conductive heat transfer in an absorbing, emitting and scattering medium, Int. J. Heat Mass Transfer 42 (1999) 2967–2980.
[25] H.P. Tan, H.L. Yi, P.Y. Wang, L.M. Ruan, T.W. Tong, Ray tracing method for transient coupled heat transfer in an anisotropic scattering layer, Int. J. Heat Mass Transfer 47 (2004) 4045–4059.
[26] H.L. Yi, H.P. Tan, Y.P. Lu, Effect of reflecting modes on combined heat transfer within an anisotropic scattering slab, J. Quant. Spectrosc. Radiat. Transfer 95 (2005) 1–20.
[27] H.L. Yi, M. Xie, H.P. Tan, Ray tracing method for radiative heat transfer within a two-layer anisotropic scattering medium, Numer. Heat Transfer Part A 54 (2008) 481–506.
[28] H.L. Yi, H.P. Tan, Transient radiative heat transfer in an inhomogeneous participating medium with Fresnel's surfaces, Sci. Chin. Ser. E 51 (2008) 1110–1124.
[29] J.F. Luo, S.L. Chang, J.K. Yang, X. Shen, G. INOUSSA, Transient coupled heat transfer in a rectangular medium with black surfaces, J. Quant. Spectrosc. Radiat. Transfer 109 (2008) 2603–2612.
[30] S.V. Patankar, Numerical Heat Transfer and Fluid Flow, McGraw-Hill, New York, 1980. Translated by Zhang Zheng, Science Press, Beijing, 1989, pp. 53–56.
[31] W.Q. Tao, Numerical Heat Transfer, Publishing Company of Xian Jiao Tong University, 1988. 145.
[32] J.F. Luo, X. Shen, Numerical method of the ray tracing-node analysing method for solving 2-D coupled heat transfer in a rectangular medium, Numer. Heat Transfer Part A 55 (2009) 456–486.